JOURNAL OF SOLID STATE CHEMISTRY **129,** 334–340 (1997)
ARTICLE NO. SC967261

Synthesis of Metastable Perovskite-type $YMnO_3$ and $HoMnO_3$

H. W. Brinks, H. Fjellvåg, and A. Kjekshus[1]

Department of Chemistry, University of Oslo, P.O. Box 1033 Blindern, N-0315 Oslo, Norway

Received August 28, 1996; in revised form December 4, 1996; accepted December 9, 1996

Metastable, orthorhombic $YMnO_3$ and $HoMnO_3$ with the perovskite-type structure have been prepared by a solution-based procedure via complexation by citrates. The crystallization process has been investigated to obtain knowledge about what happens and how to control the process. Powder X-ray diffraction, thermoanalytical, and magnetic susceptibility data have been recorded for characterization of the reaction products. The oxygen partial pressure during crystallization seems to be the parameter which largely controls the yield of the metastable modification of $YMnO_3$ and $HoMnO_3$. The inorganic precursor appears to consist of an oxide carbonate just prior to the crystallization, however, with manganese in an average oxidation state higher than 3. The crystallization does not occur during the decomposition stage unless a parallel reduction takes place. Cation-deficient o-$Y_{1-u}Mn_{1-v}O_3$ and $Ho_{1-u}Mn_{1-v}O_3$ may be formed as intermediates and enhance the amount of the o-modification in an oxidizing atmosphere.

I. INTRODUCTION

The term metastable phase is usually used for a compound which has the same composition, but a different structure than the thermodynamically stable. The system is then located in a local rather than in an overall minimum of the Gibbs free energy.

The conversion of a metastable phase to its stable modification is an irreversible process. Therefore, attempts to synthesize metastable phases frequently end up with a phase mixture containing also variable amounts of the stable modification. In order to obtain a phase-pure product of the metastable modification, control over many synthesis variables is essential.

Several requirements must be fulfilled in order to prepare a metastable compound when the ruling conditions favor the stable modification: In order to ease nucleation, the structure of the precursor phase should have more in common with the metastable than with the stable phase, the Gibbs free energy for the precursor must exceed that for the metastable phase, and the temperature must be low enough and the kinetic hindrance large enough to prevent (complete or partial) conversion into the stable state. A major challenge in synthesis of metastable compounds is hence to design a precursor with a suitable atomic arrangement. This is difficult enough in the case of crystalline precursors, but far worse for amorphous precursors.

Usually metastable phases are made by a low-temperature decomposition of a precursor, and the resulting product is mostly less dense than the stable phase. For the present oxides, Szabo (1) found that $YMnO_3$ and $HoMnO_3$ could be obtained in their orthorhombic (o), high pressure modifications (in admixture with the stable hexagonal (h) $YMnO_3$ (2)) via a solution route based on complexation with citrates. However, in this case the metastable (high pressure modification) has about 10% higher density than the thermodynamically stable phase.

The metastable $YMnO_3$ and $HoMnO_3$ phases (3, 4) have an orthorhombically deformed perovskite-type structure (space group *Pnma*); consisting of corner-sharing MnO_6 octahedra with Y or Ho in the 12-coordinated interstices. Alternatively, O and Y or Ho can be regarded as forming a cubic closed packed lattice with Mn in every fourth octahedral hole. The stable phase (5) has a hexagonal $LuMnO_3$-type structure (space group $P6_3cm$) with $ABCACB\cdots$ stacking of closed packed O layers, Mn in trigonal bipyramidal holes and Y or Ho in 7-coordinated cavities. The phase transition between the two modifications is reconstructive and of first order.

The perovskite-type structure is the thermodynamically stable structure for the rare earth (RE) manganites with the largest lanthanoides, whereas for the smallest RE the $LuMnO_3$-type structure is the stable one. In the Mn-lanthanoide series, $HoMnO_3$ is the first member with the latter structure type (5). Y^{3+} has almost the same size as Ho^{3+} (6), and $YMnO_3$ and $HoMnO_3$ take the same stable structure. Extrapolation of thermodynamic data at 1200°C for the stable compounds (7, 8) shows that the pairwise differences in Gibbs free energy between the stable and metastable modifications are relatively small for $YMnO_3$ and $HoMnO_3$.

[1] To whom the correspondence should be addressed.

0022-4596/97 $25.00

Consequently, it appears possible to synthesize metastable $YMnO_3$ and $HoMnO_3$ via a low-temperature route, e.g., based on citrate precursors. The present article reports on such attempts. The experimental conditions are primarily tested out for $YMnO_3$. The most promising synthesis conditions were thereafter adopted for $HoMnO_3$.

II. EXPERIMENTAL

Synthesis. The starting materials for the preparation of the citrate gels were Y_2O_3 (99.99%, Molycorp), Ho_2O_3 (99.0%, Fluka), $Mn(CH_3COO)_2 \cdot 4H_2O$ (99.0%, Fluka), and $C_3H_4(OH)(COOH)_3 \cdot H_2O$ (reagent grade, Sturge Biochemicals). Y_2O_3 and Ho_2O_3 were heated to 1000°C to remove water and CO_2. The Mn content of $Mn(CH_3COO)_2 \cdot 4H_2O$ was determined gravimetrically by complete decomposition to stoichiometric Mn_2O_3 at 850°C in air (9).

Y_2O_3 (or Ho_2O_3) was first dissolved in melted citric acid monohydrat [mass ratios 1:(20–100)]. $Mn(CH_3COO)_2 \cdot 4H_2O$ was added, along with some water. The water content was kept low until all Y_2O_3 was dissolved to prevent formation of (kinetically difficult dissolvable) $Y(OH)_3$. The solution was heated in a furnace at 180°C where polymerization and partial decomposition of the organic component took place. The obtained porous, X-ray amorphous xerogel (the organic precursor), was fired at 350–450°C to remove a major part of the carbonaceous species. The X-ray amorphous rest is ascribed the composition $YMnO_{3+\delta-x-y/2}(CO_3)_x(OH)_y$, where the composition variable δ is introduced to allow for a mixed III–IV valence state for Mn. Heating of this intermediate product at 600 and 700°C in air irreversibly removes some H_2O and CO_2. Combustion analyses (carried out at Ilse Beetz) of one and the same precursor heated to 350, 600, and 700°C for 24 hr gave the x and y values listed in Table 1, and the thermogravimetric curves shown in Fig. 1 refer to the same samples. The thus obtained *inorganic* precursors decompose

TABLE 1

Content of CO_2 and OH in a Selected Inorganic Precursor in Terms of Mass (m, in %) and Specified According to the Postulated Formula $YMnO_{3+\delta-x-y/2}(CO_3)_x(OH)_y$

	Element analysis					TG data	
	CO_2 content		OH content		Total		
t/°C	m	x	m	y	m	Loss t_S to t_E[a] m	Total m
350	5.8	0.28	3.2	0.74	9.0	4.2	8.6
600	5.1	0.24	1.7	0.38	6.8	4.3	6.7
700	4.1	0.19	1.1	0.24	5.2	4.2	6.2

[a] See Fig. 1, from which also numerical data were extracted.

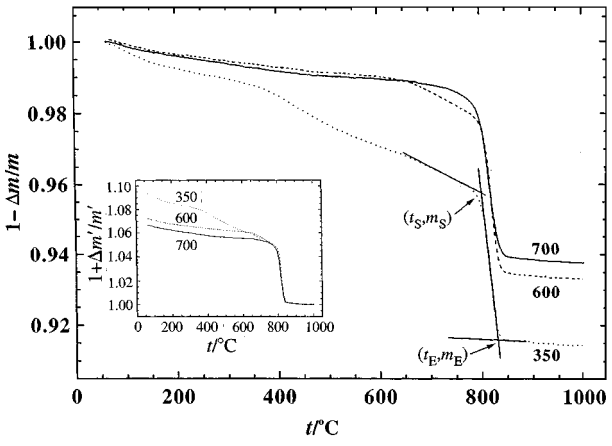

FIG. 1. TG curves for a precursor fired at 350°C for 3 hr, followed by 24-hr heat treatment at the temperatures (in °C) stated. Evaluation of start and end temperatures for decomposition of the inorganic precursor and mass loss ($\Delta m = (m_S - m_E)/m_S$) is indicated on the curve for 350°C. Inset shows the same TG data with mass change, normalized to 1.00 for the product ($YMnO_3$) at 1000°C.

at about 800°C, where crystallization also occurs. DTA measurements reveal an exotherm effect at about 800°C. A few hours heating at about 800°C is sufficient to obtain well-crystallized products.

Powder X-ray diffraction (PXD). All samples were characterized by PXD with Guinier–Hägg cameras, using Si ($a = 543.1065$ pm) as internal standard and Cu$K\alpha_1$ ($\lambda = 154.0598$ pm) radiation. All data reported refer to samples which, within detection limits, contained only o- and h-$YMnO_3$($HoMnO_3$), viz., no impurity of binary oxides.

The reflections on the PXD films were measured manually, using a comparator. Unit-cell parameters were derived by least-squares calculations using the program UNITCELL (10). The fraction of o-$YMnO_3$ was determined from relative intensities of reflections compared with mechanically made two-phase standards of o- and h-$YMnO_3$. A Nicholet LS-18 film scanner and the program SCANPI 9 (11) were used to collect intensity data.

Indexing of o-$YMnO_3$ and o-$HoMnO_3$ was carried out with the aid of intensity calculations (12) using the positional parameters for the isostructural phase $TbMnO_3$ (13). The positional parameters for $LuMnO_3$ (5) were used in a similar way to index h-$YMnO_3$. This indexing turned out to be in accordance with the JCPDS-listings except for (021) which should be (020) for o-$YMnO_3$ and (304) instead of (215) for h-$YMnO_3$.

Thermogravimetric (TG) analysis. TG measurements were carried out with a Perkin–Elmer 7 series instrument. Silica-glass containers were used as sample holders, and the heating rate was 2 K min^{-1}.

Magnetic susceptibility. Magnetic susceptibility (SQUID) measurements were performed with MPMS (Magnetic Property Measurement System; Quantum Design) and corrected for diamagnetism (14).

Infrared spectroscopy (IR). IR spectra were recorded with a Perkin–Elmer diffuse reflection instrument.

III. SYNTHESIS

During the synthesis several parameters which may influence the amount of o-$YMnO_3$ in the product are open for systematic variation. Since little is known regarding the structure (viz., atomic arrangement) of the precursor, it is important not to overlook parameters which may influence precursor properties. Altogether 15 parameters which may be of importance were identified; amount of citric acid and water, Y(Ho):Mn stoichiometry, seeding, degree of decomposition during dissolution process, drying temperature and time, storing time for organic precursor, firing temperature and time, storing time for inorganic precursor, crystallization temperature and time, crystallization atmosphere and heating rate in the crystallization region. Of these 7 were considered more important than the others and were varied, primarily one at a time, to find the optimum favorable situation with respect to amount of solvent, amount of seeding, firing temperature and time, atmosphere, temperature, and heating rate in the crystallization region.

Effect of citric acid. A wide range of solvent concentrations were tested. However, repeated syntheses under (within our control) equal conditions brought about very different results. Six individually made, expectedly identical precursors (solvent ratio 1:90) gave after intended identical treatment 26, 29, 31, 49, 53, and 79% yields of o-$YMnO_3$. For precursors with solvent ratio 1:49, 23, 38, 90, 96, and 98% were obtained. Hence, another yet unidentified synthesis parameter must be operative. In contrast, for repeated experiments with different parts of one and the same precursor, the reproducibility is fully acceptable. On this basis it was considered quite satisfactory to proceed with the evaluation of the other six selected parameters.

Effect of seeding. As a possible aid in the crystallization of o-$YMnO_3$, seeding with an isostructural phase (o-$DyMnO_3$) with nearly matching unit-cell dimensions was investigated. Three parts of an inorganic precursor were separately mixed and milled with 0, 2, and 4% of previously milled o-$DyMnO_3$ and thereafter treated at 900°C in air for 5 hr. The yields of o-$YMnO_3$ were, however, virtually identical (about 80%). In contrast, if the added o-$DyMnO_3$ acts as centers for the crystallization one may perhaps expect a lower crystallization temperature and an enhanced yield by very slow heating. However, attempts with a reduced heating rate of 5 K hr^{-1} between 720 and 800°C did not significantly change the yield of o-$YMnO_3$. The conclusion is therefore that seeding according to the present procedure is of minor significance.

Effect of firing temperature. An organic precursor was divided into three parts which were fired at three different temperatures (350, 400, and 450°C) before subjected to parallel crystallization at 900°C in air. The fractions of o-$YMnO_3$ were 85, 38, and 31%, respectively. For this reason 350°C was used in all subsequent syntheses.

Effect of firing time. TG experiments showed that on subsequent rapid heating to 350°C, constant weight was obtained after 1 hr. The real temperature of the sample during the combustion was found to be about 50°C higher than the furnace temperature. The fact that the temperature settled at the programmed temperature after 1 hr suggests that this should be sufficient also for large scale samples.

Parallel firing of portions from several precursors at 350°C (followed by crystallization at 900°C) showed that the period for the heat treatment at 350°C (here 1 to 24 hr) had no significant effect on the yield of o-$YMnO_3$. In the other experiments, all samples were consistently fired for 3 hr (which should ensure complete combustion of the organic component).

Effect of crystallization temperature. Reasonably rapid crystallization is achieved above 800°C. Temperatures above 1000°C were avoided owing to partial transformation of o- to h-$YMnO_3$. In the final experiments, 900°C was selected as crystallization temperature.

It turned possible, but rather time consuming, to crystallize $YMnO_3$ below 800°C, e.g., 2 days at 750°C, more than 3 days at 730°C, and 14 days at 700°C. Moreover, on decreasing the crystallization temperatures, decreased yields of o-$YMnO_3$ occurred. (At 700°C two extra PXD reflections which may originate from the pyrochlore-type phase $Y_2Mn_2O_7$ (15) were obtained.)

Effect of heating rate. It made no difference whether the inorganic precursor was placed in a preheated furnace or merely heated at a rate of 5 K hr^{-1}. In the subsequent experiments a preheated furnace was used.

Effect of atmosphere during crystallization. Several inorganic precursors were divided and treated identically, except for the atmosphere during crystallization. Gradual heating to 900°C in a temperature-controlled tube furnace in different O_2/N_2 mixtures (Fig. 2) and in CO_2 indicated that O_2 is favorable for the formation of o-$YMnO_3$. Parallel TG measurements (2 K min^{-1} up to 1000°C) on different precursors in various atmospheres confirmed these findings (Table 2).

Because of this clear correlation between oxygen partial pressure and the yield of o-$YMnO_3$, attempts were made to increase the oxygen partial pressure to about 7.7 bar (in

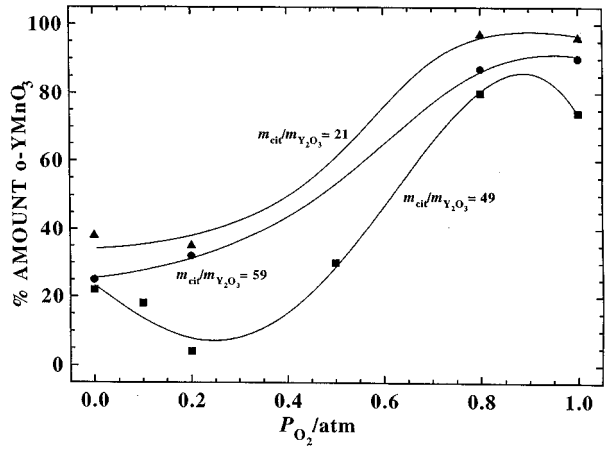

FIG. 2. Amount of o-$YMnO_3$ as a function of oxygen partial pressure for different solvent molar ratios.

a silica-glass container). However, this treatment invariably gave a mixture of o-$YMnO_3$, h-$YMnO_3$, and $Y_2Mn_2O_7$ (15, 16).

Conclusion. The present findings suggest strongly that the oxygen partial pressure seems to be the parameter with the largest influence on the yield of o-$YMnO_3$. Analogous findings were obtained for o-$HoMnO_3$.

IV. CHARACTERIZATION

Unit-cell parameters for h-$YMnO_3$, o-$YMnO_3$, and o-$HoMnO_3$ given in Table 3 agree with published data. On heating, o-$YMnO_3$ transforms to h-$YMnO_3$ within 2 hr at 1100°C in air, whereas o-$HoMnO_3$ is only partially converted to h-$HoMnO_3$ after two days at 1250°C.

TABLE 2
Results from TG Experiments for Different Selected Precursors (2 K min^{-1})[a]

Precursor	Atmosphere	t_S/°C	t_E/°C	Δm/%	o-$YMnO_3$/%[b]
1	Air	809	836	− 4.1	94
1*	Air	803	829	− 4.2	98
1†	Air	806	832	− 4.3	95
1‡	Air	799	832	− 4.2	97
1	O_2	835	866	− 4.2	99
1**	O_2	820	847	− 4.4	99
1	N_2	773	801	− 3.6	30
1	CO_2	775	803	− 3.7	35
2	Air	800	838	− 2.6	28
2	CO_2	758	801	− 1.9	0
3	Air	792	834	− 2.7	52
3	N_2	765	804	− 2.0	10
4‡	Air	800	837	− 2.2	40
4‡	CO_2	654	691	− 4.5	0
5	Air	788	831	− 2.4	5
6	Air	798	838	− 2.1	55
7	Air	787	826	− 4.2	92

[a] The temperatures where the mass loss during crystallization starts (t_S) and ends (t_E), the size of the mass loss (Δm) relative to the mass where it starts, and the amount of o-$YMnO_3$ in the product after cooling in air. All precursors are annealed at 350°C for 3 hr except for *31 additional hours at 350°C, † 1 additional day at 600°C, ‡ 1 additional day at 700°C, and **40 additional hours at 350°C. Additional data for precursor 1 are found in Fig. 1 and Table 1.

[b] Balance: h-$YMnO_3$.

[c] Differs from other precursors by a content of residual coal. This gave an additional mass loss at 400°C in air and a very individual TG curve in CO_2.

The magnetic susceptibility for h- and o-$YMnO_3$ (Fig. 3) follows Curie–Weiss law above 200 and 100 K, respectively. Magnetic parameters (Table 3) are consistent with values found in the literature. The shape of the $\chi^{-1}(T)$ curve for

TABLE 3
Unit-Cell Dimensions (*Pnma* for o-$YMnO_3$ and o-$HoMnO_3$, $P6_3cm$ for h-$YMnO_3$) and Magnetic Data

	Crystallographic data				Magnetic data		
Compound	a/pm	b/pm	c/pm	$V/Z \cdot 10^7$ pm^3	μ_p/μ_B	θ_p/K	Ref.
h-$YMnO_3$	613.92(6)		1140.0(1)	6.2017(6)	5.91(2)[a]	− 578(24)[a]	Present
	612		1139		5.37[b]	− 550[b]	16[c]
o-$YMnO_3$	582.6(2)	736.1(2)	525.4(2)	5.628(2)	4.70(2)[a]	− 14(2)[a]	Present
	584	736	524		4.98[b]	− 67[b]	16[c]
h-$HoMnO_3$	614.2(3)		1141.7(7)	6.217(6)			Present
	613		1143				16[c]
o-$HoMnO_3$	582.2(2)	736.7(2)	526.0(2)	5.640(2)	11.89(1)[d]	− 17.0(1)[d]	Present
	584	735	526		11.3[b]	− 23[b]	16[c]

Note. Calculated standard deviations are in parentheses.

[a] Measuring field 0.1 kOe.

[b] Measuring field 5.7–10.1 kOe.

[c] Virtually identical unit-cell parameters are given in Refs. 3–5.

[d] Measuring field 1.0 kOe.

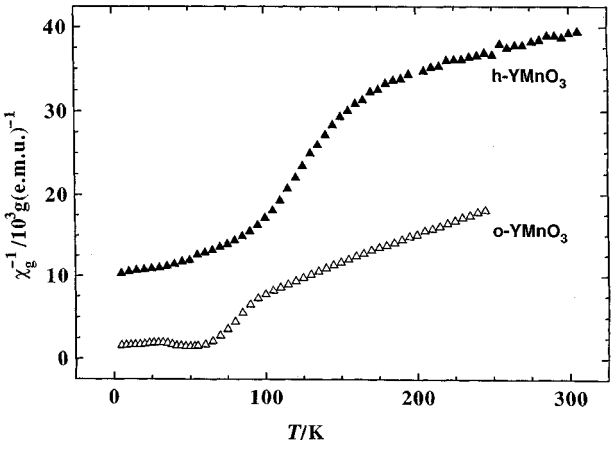

FIG. 3. Inverse magnetic susceptibility for o-$YMnO_3$ and h-$YMnO_3$ at 0.1 kOe.

o-$YMnO_3$ in a 0.1-kOe field resembles that in Ref. (17) below the Curie–Weiss region. However, it should be noted that the curve shape to some extent depends on the measuring field (evidenced by field scans (0.1–35 kOe) at 5 K in this study). This may indicate small amounts (≤ 1 wt‰) of ferrimagnetic Mn_3O_4 impurities (18), although the adopted 5-hr treatment at a maximum temperature of 830°C in the synthesis of the measured sample should certify that any precipitation of Mn surplus should turn up as antiferromagnetic Mn_2O_3 (19) rather than ferrimagnetic Mn_3O_4.

The $\chi^{-1}(T)$ curves of o-$HoMnO_3$ follows Curie–Weiss law above 20 K. The increase below 6.5 K (Fig. 4) is probably due to antiferromagnetic ordering of the Ho moments.

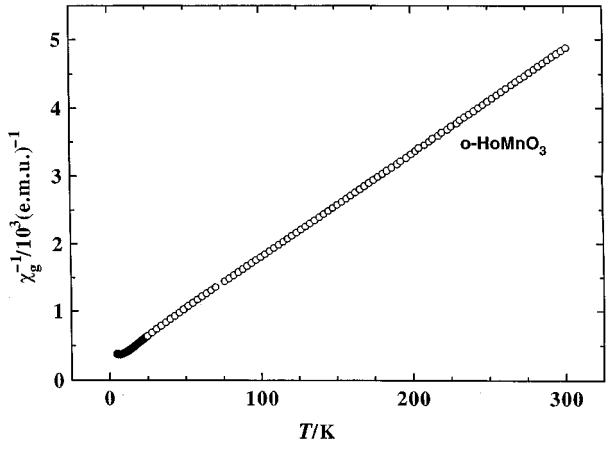

FIG. 4. Inverse magnetic susceptibility for o-$HoMnO_3$ at 1.0 kOe.

V. ON THE CRYSTALLIZATION PROCESS

All inorganic precursors prepared in this study differ somewhat; above all they did not have a well-defined composition in terms of x and y, and none of them were obtained in a crystalline state. However, there seemed to be only minor differences according to the relatively featureless IR spectra between inorganic precursors which give much and little o-$YMnO_3$ on crystallization at 900°C in air.

The experimental data indicate the following situation during the crystallization: The inorganic precursor appears to consist of an amorphous oxide carbonate just prior to crystallization, however, with manganese in an average oxidation state higher than 3. The crystallization does not occur during the decomposition unless a parallel reduction takes place. In a reducing atmosphere this happens prior to decomposition, whereas under oxidizing conditions the reduction and decomposition appear to be coupled. In the latter case, o-$Y_{1-u}Mn_{1-v}O_3$ may be formed as an intermediate state and cause an increased amount of o-$YMnO_3$ in an oxidizing atmosphere. Our arguments in favor of this view are mostly based on TG experiments, on different precursors, and in different atmospheres (Fig. 1 and Table 2).

The decomposition (temperature and relative mass loss) of a given precursor is clearly dependent on the atmosphere. In N_2 as well as CO_2 the decomposition temperature is 30–40°C lower than in air, which in turn is lower than in O_2. The mass loss is invariably some 0.5% larger in air and in O_2 than in CO_2 and in N_2, but the crystalline product has the same unit-cell dimensions and hence stoichiometry regardless of the atmospheres (in accordance with Ref. (7)). Preannealing at different temperatures did not resolve the origin of this mass discrepancy. The difference is not caused by deposition of coke under nonoxidizing conditions, as proven by TG experiments on crystallization in N_2 and subsequent reheating in O_2.

We thus arrived at the opinion that the difference in behavior may result from manganese being in a higher average oxidation state than 3 in the inorganic precursor. The mass difference of about 0.5% corresponds to a content of about 14% Mn(IV) in the inorganic precursor. In CO_2 and N_2 atmospheres the decomposition temperature of the thus reduced oxide carbonate is the limiting factor, whereas in air and O_2, the reduction temperature is of importance.

This view is further supported by the observation that crystallization at low temperature or high oxygen partial pressures gives a mixture of $Y_2Mn_2O_7$ together with $YMnO_3$; viz., the crystallization has occurred without a reduction of the manganese. One can envisage the incorporation of both Mn(III) and Mn(IV) in an oxygen excessive $YMnO_{3+\delta}$ phase (like $LaMnO_{3+\delta}$), although, as observed, such a phase is not stable (see also Ref. (7)). However, one may imagine an intermediate with these features.

Furthermore, we are convinced that the inorganic precursor is not in equilibrium prior to the decomposition. Therefore the crystallization process is mainly controlled by kinetics.

First, TG and DTA indicate that decomposition and crystallization happens simultaneously at about 800°C, and the overall process is exothermic. Second, crystalline $YMnO_3$ is obtained after heating at 700°C for two weeks. This is about 100°C lower than the crystallization temperature obtained under dynamic conditions. Third, one is faced with the fact that a more CO_2-rich atmosphere lowers the decomposition and crystallization temperature. (This observation contradicts the prediction by Le Chateliers principle for an assumed oxide carbonate precursor and lends apparently additional support to the kinetics hypothesis. For comparison it may be mentioned that we observe a rise in the temperature of formation of Y_2O_3 from 750 (in air) to 980°C (in CO_2) by heating yttrium citrat via $Y_2O_2CO_3$.)

Our conclusion is that the mentioned explanation seems to be reasonable and that the oxidation power of the atmosphere rules the kinetics of the crystallization.

VI. METASTABILITY OF o-$YMnO_3$

o-$YMnO_3$ appears to be metastable under the given synthesis conditions. The Gibbs energy differences, relative to MnO and Y_2O_3, for h- and o-$YMnO_3$ at 1200°C, are -47.7 and -43.9 kJ/mol, respectively (7, 8). The value for o-$YMnO_3$, not even being kinetically stable at 1200°C, is linearly extrapolated from the series $REMnO_3$ (RE = La, Pr, Nd, Sm, Dy) (7, 8). Unless there is a large degree of disorder in h-$YMnO_3$, it appears improbable that $\Delta G(T)$ can change so much that o-$YMnO_3$ becomes the stable phase at the synthesis temperature of 800°C. Changes in h-$YMnO_3$ other than a gradual tilting of the Mn coordination polyhedra are not reported, and these known alterations are certainly not enough to significantly modify the stability. On this basis we conclude that h-$YMnO_3$ is stable relative to o-$YMnO_3$ in the temperature range concerned.

VII. CONCLUDING REMARKS

The experiments show that the redox properties have a large influence on the product. There are mainly three ways to control the progress of a redox reaction of this kind: Oxygen partial pressure, temperature, and admixture of an oxidizing agent (ultimately removable from the product). The crystallization temperature represents the lower temperature limit, and oxygen partial pressures ranging between 10^{-4} and 92 bar have been tested. Above some 2–6 bar, Mn adopts an oxidized state $>$ III. Hence, attempts to vary the temperature and/or oxygen partial pressure appear to suggest that these variables are not the right tools to further increase the amount of o-$YMnO_3$ in the product. Tests with HNO_3 as an oxidizing agent did not give a positive effect, and other suitable reagents were not found.

There is a striking similarity between the syntheses of $YMnO_3$ and $HoMnO_3$ on the one hand, and $ScMnO_3$ [Tl_2O_3-type structure (20)] on the other, in that the metastable modifications of these compounds possess six-coordinated Mn, while the stable modifications contain five-coordinated Mn. This may possibly be of significance, but more insight is needed in order to establish a link between the complexations in citrates and six-coordinated Mn. It should be well documented that small structural differences in inorganic precursors control the crystallization, and that such factors are more important than the efficient utilization of volume in the product (note the enlarged density for the metastable modification in the present case). The problem is, however, that the structure of the precursors are unknown.

Maintaining that the atomic arrangement of the precursor is of utmost importance for the successful synthesis of a metastable phase (provided that other conditions are satisfied), it would be of great help to be able to perform parallel synthesis along a different route. However, this is not always easy, if at all possible.

Even for a crystalline precursor it is far from straightforward to predict the structure of its decomposition product. A good example in this respect is the well-known synthesis of TiO_2(B) from $Ti_4O_7(OH)_2 \cdot 4H_2O$ (21). From the knowledge of the TiO_2-anatase (21) and TiO_2(B) (21) structures, it is not obvious that the decomposition of $Ti_4O_7(OH)_2 \cdot 4H_2O$ should lead to the latter rather than the former modification of TiO_2. For an amorphous precursor such predictions are much more speculative.

As a final summary it can be said that synthesis of metastable compounds in only a very few cases can be planned, and in order to work out a useful strategy a huge amount of knowledge about the stable and metastable phase as well as the precursor is required. It is in fact much more likely that one will come across a metastable phase by accident and then optimize its synthesis procedure afterward.

ACKNOWLEDGMENT

H. W. Brinks is grateful to The Research Council of Norway for financial support.

REFERENCES

1. G. Szabo, Thèse University of Lyon, Lyon, France 1969.
2. S. Quezel, J. Rossat-Mignod, and E. F. Bertaut, *Solid State Commun.* **14,** 941 (1974).
3. A. Waintal and J. Chenavas, *C. R. Acad. Sc. Paris* **264,** 168 (1967).
4. A. Waintal and J. Chenavas, *Mater. Res. Bull.* **2,** 819 (1967).

5. H. L. Yakel, W. D. Koehler, E. F. Bertaut, and F. Forrat, *Acta Crystallogr.* **16,** 957 (1963).
6. R. D. Shannon, *Acta. Crystallogr. Sect. A* **32,** 751 (1976).
7. K. Kamata, T. Nakajima, and T. Nakamura, *Mat. Res. Bull.* **14,** 1007 (1979).
8. V. A. Cherepanov, L. Yu. Barkhatova, and A. N. Petrov, *J. Phys. Chem. Solids* **55,** 229 (1994).
9. F. Shenouda and S. Azuz, *J. Appl. Chem.* [*London*] **17,** 258 (1967).
10. B. Noläng, Program UNITCELL, Version 1.0, Institute of Chemistry, University of Uppsala, Uppsala, Sweden, 1990.
11. P. E. Werner, Program SCANPI, Version 9, Institute of Inorganic Chemistry, University of Stockholm, Stockholm, Sweden, 1992.
12. K. Yvon, W. Jeitschko, and E. Parthé, *J. Appl. Crystallogr.* **10,** 73 (1977).
13. S. Quezel-Ambrunaz, *Bull. Soc. Franç. Minér. Crist.* **91,** 339 (1968).
14. P. W. Selwood, "Magnetochemistry," 2nd ed., Interscience, New York, 1956.
15. M. A. Subramanian, C. C. Torardi, D. C. Johnson, J. Pannetier, and A. W. Sleight, *J. Solid State Chem.* **72,** 24 (1988).
16. H. W. Brinks, A. Kjekshus, and H. Fjellvåg, to be published.
17. V. E. Wood, A. E. Austin, E. W. Collings, and K. C. Brog, *J. Phys. Chem. Solids* **34,** 859 (1973).
18. K. Dwight and N. Menyuk, *Phys. Rev.* **119,** 1470 (1960).
19. E. Sonder, *Oak Ridge Natl. Lab.* **17,** 2614 (1958).
20. P. Karen, H. Fjellvåg and A. Kjekshus, to be published.
21. M. Tournoux, R. Marchand, and L. Brohan, *Prog. Solid St. Chem.* **17,** 33 (1986).